Bulk and surface electron emission induced by ion bombardment: methods of observation



1991 J. Phys.: Condens. Matter 3 8289

(http://iopscience.iop.org/0953-8984/3/42/023)

J. Phys.: Condens. Matter 3 (1991) 8289–8296. Printed in the UK

# Bulk and surface electron emission induced by ion bombardment: methods of observation

W Soszka
Institute of Physics, Jagellonian University, Kraków, Poland

Received 29 October 1990, in final form 21 March 1991

**Abstract.** It was found that the energy spectrum of secondary electrons emitted under ion bombardment of the cold (below 100 K) metal targets contains an additional maximum, the position of which on the energy scale depends on the ion incidence angle and the angle of electron detection. This maximum is also observed at room temperature but only at grazing exit angles. The additional maximum is supposed to be a result of the creation of electrons on the surface. Such electrons can be distinguished from the bulk electron emission at the special experimental arrangement (low target temperature and small exit angle of electrons).

## 1. Introduction

During the ion penetration of solids, part of the kinetic energy of the ions is transferred to the bonded and free electrons and they can leave the target (ion-induced kinetic electron emission). In the energy region of about 10 keV (low-energy ion spectroscopy (LEIS) region) the heavier projectiles (ions or fast recoils) are exposed to a few violent collisions and a large number of weak and very weak collisions. Usually, the path between two violent collisions is short and inelastic losses of energy which are accumulated during this path due to weak collisions do not exceed the ionization energy of the projectile. For the heavier projectiles the mechanism of kinetic emission connected with weak collisions can be neglected in contrast with the light projectiles for which the cross section for scattering is small and the path between violent collisions is much longer. Thus, the main sources of electrons are a short series of asymmetric (ion and target atom interactions) and symmetric (recoil and next target atom interactions) violent collisions.

During collision the electron clouds of the colliding partners interact with each other and, as the electron levels are shifted and broadened, the projectile plus recoil atom can be treated as a quasimolecule. The quasimolecule model has been introduced to describe the ion interaction with gaseous targets (Gerber *et al* 1972) but it is also helpful in the case of solid targets (Benazeth 1982). Two mechanisms of electron emission can be distinguished when the isolated quasimolecule is created. The first is a direct ionization process when, as the colliding partners approach each other, some electrons are promoted above the vacuum level (Barat and Lichten 1972). The electrons which are liberated during such a process have a continuum energy spectrum from nearly zero (maximum yield) to a few tens of electronvolts (Ogurtsov 1972). The second mechanism is connected with inner- and outer-shell excitations of the symmetric and asymmetric quasimolecules. The decays of such states take place, usually, as the collision partners recede (Soszka *et al* 1989a).

For both light and heavy projectiles the first violent collision can take place on the target surface or in the bulk, i.e. deeper than the mean free path of electrons (including elastic and inelastic electron scattering). In the last case the electrons do not conserve the energy and momentum which they have at the moment of origin and they create bulk electron emission with a characteristic energy distribution (resembling the Maxwellian curve) and cosine angular distribution. If the electron excitation takes place on the surface or near to the surface, then a relation between the energy of electron and its momentum can be conserved and the surface electrons may be visible as some structure of the energy spectrum under the condition that the yield of bulk electrons will be restricted. A decrease in the yield of bulk electrons may be realized in the grazing exit geometry or by low target temperatures. Both cases are considered in the presented paper.

## 2. Experimental details

The experimental set-up has been described elsewhere (Budzioch *et al* 1986). The polycrystalline Au target or crystalline Ni(100) target were mounted on a two-axis goniometer placed in a vacuum chamber with a residual gas pressure in the range of $6 \times 10^{-10}$–$2 \times 10^{-9}$ Torr during operation. The target holder was connected, by copper

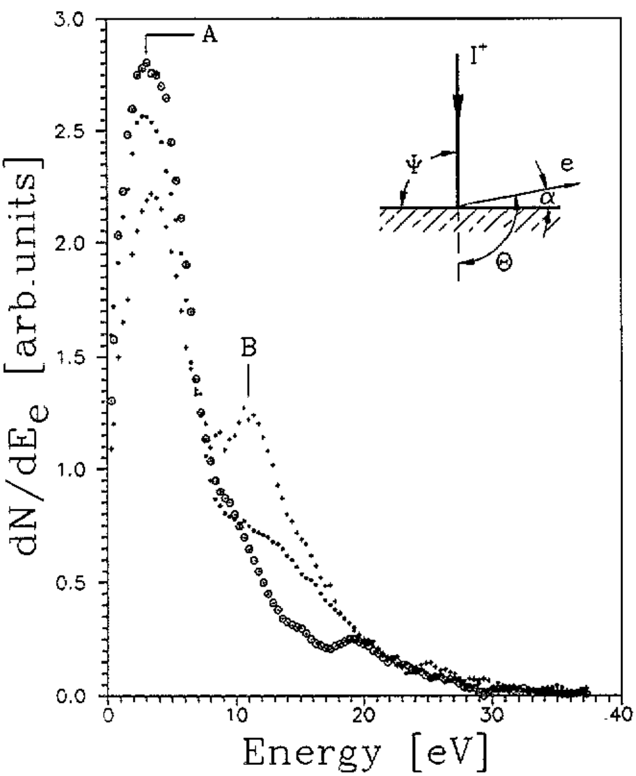


**Figure 1.** Energy spectra of secondary electrons emitted from the polycrystalline Au target upon bombardment with 7 keV $Ne^+$ ions at different combinations of detection angles $\Theta$ and ion incidence angles $\Psi$: $\odot$, $1-\Theta = 80°$, $\Psi = 75°$; $*$, $\Theta = 85°$, $\Psi = 80$; $+$, $\Theta = 90°$, $\Psi = 85°$. The outlet angle of electrons, i.e. $\alpha = \Theta - \Psi = 5°$, was constant. The inset is a schematic illustration of the geometrical arrangement of the target.

braids, with the cold finger of the flow helium cryostat. The $Ne^+$ ion current was measured with a movable Faraday cup and was about 10 nA. The rotatable electron detection system consists of a cylindrical energy analyser with an energy resolution of about 3% and an angular resolution of $\pm 0.5°$ and a channeltron multiplier as a detector. The influence of a stray magnetic field on the slowly moving electrons was suppressed by accelerating the electrons prior to their entering the electrostatic analyser. Inside the chamber the target was cleaned by argon sputtering. The state of the target surface was monitored by the LEIS method (Soszka *et al* 1989b) and no contaminant structure of the energy spectrum of 1.6 keV $He^+$ reflected from the target surface was found.

## 3. Results and discussion

The energy spectra of secondary electrons emitted from the polycrystalline Au target upon bombardment with 7 keV $Ne^+$ ions at the three detection angles ($\Theta = 90°$, 85° and 80°, respectively) and at room temperature are presented in figure 1. The ion incidence angle $\Psi$ varies in a way that the exit angle of electrons given by $\alpha = \Theta - \Psi = 5°$ is constant. The spectrum for $\Theta = 90°$ consists of two maxima A and B; however, a second maximum B is slightly visible at the smaller detection angle.

The electron energy spectra at a fixed detection angle $\Theta$ are presented in figure 2. The outlet angle of electrons changes from $\alpha = 5°$ to 15°. The strong increase in the maximum A with increase in $\alpha$ obscures maximum B.

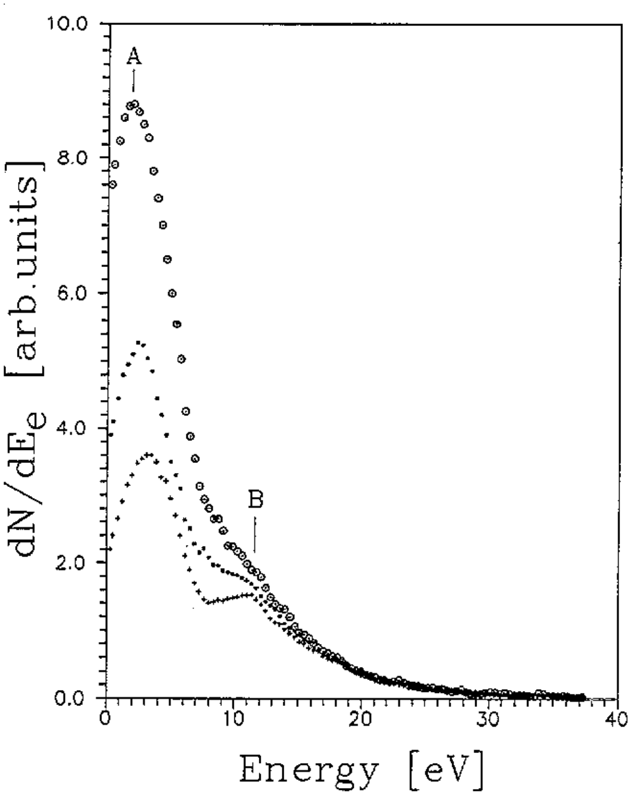


**Figure 2.** The same as for figure 1 but for the fixed detection angle $\Theta = 94°$, at different ion incidence angles: ⊙, $\Psi = 80°$; $*$, $\Psi = 85°$; +, $\Psi = 89°$.

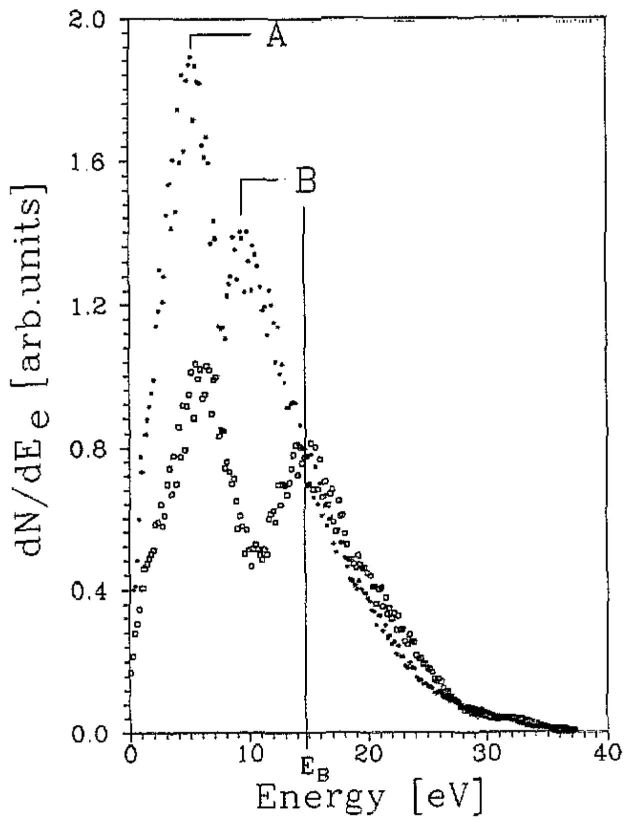


**Figure 3.** Energy distributions of secondary electrons emitted from the Ni(100) surface bombarded with 5 keV $Ne^+$ ions ([110] azimuth) at the two target temperatures: $*$, 300 K; □, 80 K. The ion incidence angle and detection angle were 85° and 90° respectively.

In figure 3 the energy distributions of secondary electrons emitted from the Ni(100) surface bombarded with 5 keV $Ne^+$ ions are presented at the two target temperatures (300 and 80 K). It can be seen that, with decreasing temperature, peak B shifts to higher energies and becomes more pronounced.

In figure 4 the energy $E_B$ of peak B as a function of the ion incidence angle $\Psi$ is shown for the 5 keV $Ne^+$–Ni interaction. In contrast with the target at room temperature, peak B for the cold target is visible over a large region of $\Psi$ (50–90°) and it shifts to higher energies with increasing incidence angle.

The maximum A is a typical maximum of the bulk electron emission. It is suggested that peak B is connected with electrons which originate at the surface. This is based on the following general considerations. The surface electron fraction in the total electron emission should occur more distinctly when the bulk emission is reduced. Indeed, for targets at room temperature, peak B is observed only at the grazing exit geometry when because of the cosine law the yield of bulk electrons is limited. With decreasing temperature the target transparency (together with the ion penetration depth) increases and that is why the yield of bulk electrons decreases for cold targets (Soszka 1991). Analysis of the behaviour of peaks A and B (figures 3 and 4) is consistent with this.

Now we consider the problem of surface and bulk electron emission in detail. The condition of scattering of electrons by the surface potential barrier (Schou 1980) is given as $E_2 \sin^2 \alpha_2 = E_1 \sin^2 \alpha_1 - U(1)$, where $E_1$ is the kinetic energy of an electron in the

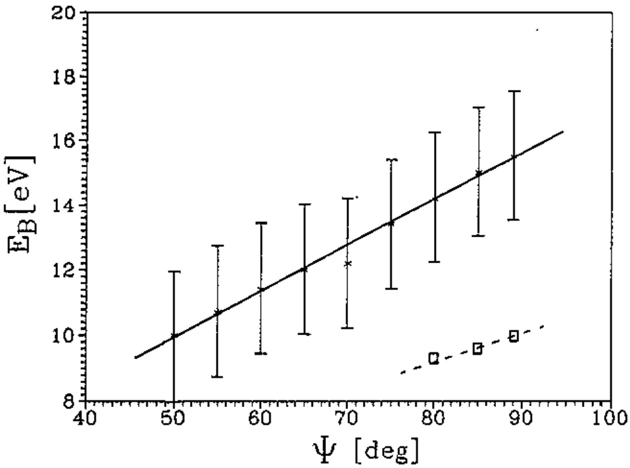


**Figure 4.** Energy position of peak B from figure 3 as a function of the incidence angle $\Psi$ at the two target temperatures: □, 300 K and ×, 80 K. The detection angle was $\Theta = 90°$.

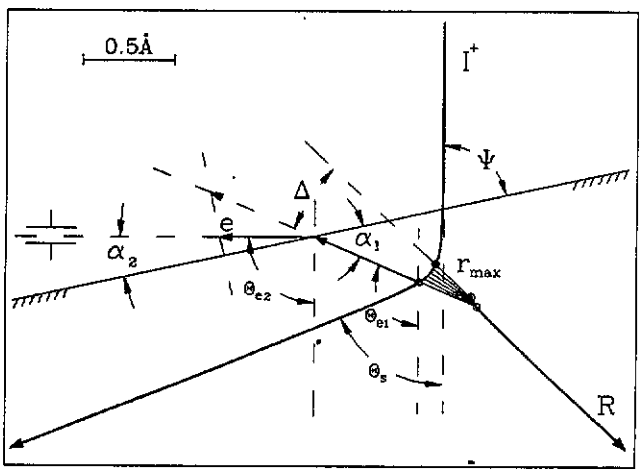


**Figure 5.** Simulated position of the $Ne^+ + Ni$ quasimolecule at which the inelastic energy losses reach a maximum. The path of the electrons through the surface barrier is also presented in this figure (schematically).

medium, $\alpha_1$ is the incidence angle of an electron inside the medium, $E_2$ is the kinetic energy of an electron in vacuum, $\alpha_2$ is the outlet angle of the electron and $U$ is the work function for the target material (figure 5; here $\alpha = \alpha_2$ and $\Theta_{e2} = \Theta$). The electrons leaving the target at a very small exit angle ($\alpha_2 \rightarrow 0$) must have had a kinetic energy $E_1 = U/\sin^2 \alpha_1$ before scattering by the surface potential barrier. If the angular distribution of secondary electrons inside the target material is isotropic and their energy spectrum is wide, then some electrons always fulfil the surface barrier condition and will be detected outside the target. If the energy spectrum of electrons is wide but the angular distribution is anisotropic (some angle $\Theta_{e1}$ of electron generation is preferred), then there is a limitation for the energy $E_{01}$ and electrons with kinetic energy $E_1 < E_{01}$ will be reflected by the surface barrier. Experimentally, this means that the electrons with energy $E_2 < E_{01} \cos^2 \alpha_1$, where $\alpha_1$ is the preferred electron incidence angle and $\alpha_1 = \Theta_{e1} - \Psi$, will be discriminated in the energy spectrum and the cut-off will occur at lower energies. If the energy spectrum is narrow and the angular distribution is anisotropic, then only for a particular detection angle can the electrons be detected outside the target and they give a peak in the energy spectrum.

There are two cases of violent collisions in which the secondary electrons are created: one is when the violent collisions are a source of electrons in the bulk and the other is when such collisions take place on the surface or near to the surface. In the first case the created electrons have a relatively long path inside the target material and owing to elastic and inelastic scattering processes change their energies and momenta. These electrons come to the surface with an isotropic angular distribution and with a wide energy spectrum and some of them fulfil the surface barrier condition, also at small outlet angles. However, according to the cosine law the number of such electrons is very small. The other situation is when electrons are created in the violent collisions near the surface. It is reasonable to assume that in this case the angular distribution of electrons will be anisotropic and their energy discrete. These electrons after scattering by the surface barrier create a peak which is visible at the determined detection angle $\Theta_{e2}$ (see above). Thus, for $E_1$ = constant, $\Theta_{e1}$ = constant and $\Theta_{e2} = \Theta = 90°$ (angle of detection) we can find the curve which corresponds to the experimental points $E_B(\Psi)$ presented in figure 4. The best fit (full line) was found to be when $E_1 = 17.5$ eV and $\Theta_{e1} = 107°$. In the above considerations the increase in the work function with decreasing $\Psi$ was taken into account. The work function depends on the number of vacancies induced by ion bombardment and changes with incidence angle and temperature. The data presented in figure 4 suggest that the work function can alter for two different temperatures: $\Delta U = \sin^2\alpha_2(E_{B80} - E_{B300})/(1 + \sin^2\alpha_1) \sim 0.1$ eV. Here $E_B$ is the kinetic energy of electrons which are liberated in the inner-shell autoionization processes during the existence of the $Ne^+$ + Ni quasimolecule. Such a conclusion can be drawn from the analysis of figure 1 where $E_B$ distinctly depends on the detection angle $\Theta_{e2}$. As has been shown by Soszka *et al* (1989a) for the molecular inner-shell autoionization processes the liberated kinetic energy is $E_k = E_B = (E_V - \Delta E) - 2U$ at normal electron incidence or $E_B = \{[(E_V - \Delta E) - U]\sin^2\alpha_1 - U\}\sin^{-2}\alpha_2$ in other cases, where $E_V$ is the binding energy of electron in the subshell V in which the initial vacancy is created during previous direct ionization or excitation, $\Delta E$ is the energy correction due to the change in the potential energy according to the correlation diagram of interaction (Barat and Lichten 1972), and $E_k$ varies with the detection angle $\Theta$. The relation between $E_k$ and $\Theta$ observed in figure 1 means that the energy and trajectory of electrons have not been perturbed by electron scattering processes and it is possible only in the case when the electrons originate near to the surface.

Now we try to consider the physical reason for the obtained value of $\Theta_{e1}$. Soszka *et al* (1989a) suggested that for heavy recoils the electrons that are created owing to a decay of outer- and inner-shell excitation states of the quasimolecule show some symmetry relative to the axis of the ion beam. The escape of electrons from the quasimolecule is realized mainly in the direction parallel to its actual long axis at the moment of decay of excited states. On the other hand, as was suggested by Parilis *et al* (1988) the inelastic energy losses reach a maximum at the internuclear separation $r_{max}$ ($r_{max} > r_0$ where $r_0$ is the distance of closest approach in the head-to-head collision) which can be found from the condition: $(d\varepsilon_{in}/dr)_{r=r_{max}} = 0$ (here $\varepsilon_{in}$ is the inelastic energy loss according to Kishinevsky (1962)). The calculations (Parilis *et al* 1988) were performed for the Thomas–Fermi potential (Torrens 1972) with the Moliere (1947) approximation and the Firsov (1957) screening length. They show that for the interaction (5 keV) $Ne^+$–Ni the distance $r_{max}$ is 0.285 Å and the scattering angle $\Theta_s$ (figure 5) is 68°. Since the yield of electrons is proportional to $I_e \sim \pi\varepsilon_{in}p^2/I_{av}$ where $p$ is the impact parameter and $p =$

$(r^2 - r_0^2)^{1/2}$ and $I_{av}$ is the average ionization potential of inner shell of atomic core, most electrons leave the scattering centre when $\varepsilon_{in}$ reaches a maximum, i.e. at the angle $\Theta_{e1} = \zeta - \Delta$, where $\zeta$ is the angle describing the direction of the long axis of the quasimolecule at the moment of closest approach $r_{max}$ (relative to the ion beam) and $\Delta$ is the angle of rotation of the quasimolecule during the de-excitation time $\tau$. The simulated position of the $Ne^+$ + Ni quasimolecule at the moment of closest approach and after a time $\tau = 10^{-16}$ s (here $\tau$ is the molecular Auger transition time (Budzioch *et al* 1986) is shown in figure 5. The angles $\zeta$ and $\Delta$ are 133° and 20°, respectively (Robinson and Torrens 1974), and finally $\Theta_{e1} = 113°$. This approximately agrees with the value of $\Theta_{e1}$ estimated from the experimental data (unfortunately, $\tau$ is not known more precisely). The obtained result confirms the assumption about anisotropic distribution of electrons and also, indirectly, that peak B in figures 1–3 can be treated as the maximum of the energy distribution of the surface electrons.

From the above-mentioned model we can try to analyse the angular dependences observed in figures 1 and 2. The existence of the surface barrier means that, at the detection angle $\Theta_{e2} < 90°$, only electrons generated at a smaller angle than $\Theta_{e1} = 107°$ or with a kinetic energy below $E_1 = 17.5$ eV can be recorded as a surface peak B. As was mentioned above, the generation angle $\Theta_{e1} = 107°$ is preferred and in other directions the yield of electrons decreases. Also because of the relation between the generation angle and the kinetic energy with decreasing $\Theta_{e1}$, the kinetic energy $E_1$ of electrons increases and the surface barrier condition cannot be fulfilled. Thus, with decreasing detection angle $\Theta_{e2}$ and at fixed exit angle $\alpha_2$, peak B should decrease and shifts to higher energies. The results presented in figure 1 confirm this.

If the detection angle $\Theta$ is fixed, then the change in ion incidence angle $\Psi$ causes a change in scattering conditions on the surface barrier. With decreasing $\Psi$ the kinetic elecron energy decreases and peak B shifts to peak A. This is especially visible for cold targets. Simultaneously, according to the cosine law ($I_e \sim \cos(\pi/2 - \Theta + \Psi)$) the bulk electron emission (peak A) strongly increases and it can cover the effect of surface electron emission (peak B in figure 2).

## 4. Conclusion

It is possible to distinguish the surface from the bulk electron emission if we assume that for the surface electrons the relation between their energies and momenta at the moment of creation is conserved. Then, for metallic targets and in the special experimental arrangement (observation at a small outlet angle, and a low target temperature) the surface electrons give some structure in the energy spectrum which can be visible on the background of bulk electrons if they are restricted or are due to scattering by the surface potential barrier or by an increase in the ion penetration depth. The experiments confirm this, which means that in the LEIS energy region the quasimolecule model which is applied to gaseous targets is also correct for solid targets.

## References

Barat M and Lichten W 1972 *Phys. Rev.* A **6** 211
Benazeth N 1982 *Nucl. Instrum. Methods* **194** 405
Budzioch J, Soszka M and Soszka W 1986 *Nucl. Instrum. Methods* B **14** 530

Firsov O B 1957 *Zh. Eksp. Teor. Fiz.* **33** 696
Gerber G, Morgenstern R and Niehaus A 1972 *J. Phys. B: At. Mol. Phys.* **5** 1396
Kishinevsky L M 1962 *Izv. Akad. Nauk SSSR Ser. Fiz.* **26** 1410
Moliere G 1947 *Z. Naturf.* a **2** 133
Ogurtsov G N 1972 *Rev. Mod. Phys.* **44** 1
Parilis E S *et al* 1988 *Atomic Collisions in Gases and on the Surface of Solids* (Tashkent: FAN) (in Russian)
Robinson M T and Torrens J M 1974 *Phys. Rev.* B **9** 5008
Schou J 1980 *Phys. Rev.* B **22** 2141
Soszka W 1991 *Nucl. Instrum. Methods* B at press
Soszka W, Kwaśny S, Budzioch J and Soszka M 1989a *J. Phys.: Condens. Matter* **1** 1353
—— 1989b *Phys. Lett.* **138A** 531
Torrens J M 1972 *Interatomic Potentials* (New York: Academic)